Age-Gain-Dependent Random Access for Event-Driven Periodic Updating

Yuqing Zhu, Yiwen Zhu, Aoyu Gong, Yan Lin, *Member*, *IEEE*,
Yuan-Hsun Lo, *Member*, *IEEE*, and Yijin Zhang, *Senior Member*, *IEEE*

***Abstract*—This paper considers utilizing the knowledge of age gains to reduce the average *age of information* (AoI) in random access with event-driven periodic updating for the first time. Built on the form of slotted ALOHA, we require each device to determine its age gain threshold and transmission probability in an easily implementable decentralized manner, so that the contention can be limited to devices with age gains as high as possible. For the basic case that each device utilizes its knowledge of age gain of only itself, we provide an analytical modeling by a multi-layer *discrete-time Markov chains* (DTMCs), where an external DTMC manages the jumps between the beginnings of frames and an internal DTMC manages the evolution during an arbitrary frame, for obtaining optimal fixed access parameters offline. For the enhanced case that each device utilizes its knowledge of age gains of all the devices, we require each device to adjust its access parameters for maximizing the estimated network expected AoI reduction per slot, through maintaining the a posteriori joint probability distribution of local age and age gain of an arbitrary device in a Bayesian manner. Numerical results validate our study and demonstrate the advantage of the proposed schemes over other schemes.**

***Index Terms*—Internet of Things, age of information, periodic update, random access, slotted ALOHA.**

I. Introduction

A. Background

Internet of Things (IoT) systems have been widely applied in many real-time services [1]–[3], such as emergency surveillance, target tracking, process control, and so on. In these services, destinations are interested in the status of one or multiple processes observed by multiple sources, and then take necessary actions based on the received status updates. To ensure the quality and even safety of these services, it is typically necessary for sources to deliver their generated updates to the corresponding destinations as timely as possible.

However, such timeliness requirement *cannot* be characterized adequately by conventional performance metrics (e.g. throughput and delay). For example, when the throughput is large, the received updates may not be fresh due to long delay; when the delay is small, the received updates may not be fresh due to infrequent arrivals of updates. As such, a new performance metric, termed *age of information* (AoI), has been introduced in [4] to measure the time elapsed since the generation moment of the latest successfully received update at a destination. Naturally, to reduce the network *average AoI* (AAoI), it is desirable for multiple access schemes to assign higher transmission priorities to devices with higher age gains, where the age gain of a device in a slot quantifies how much a successful transmission of this device will reduce its corresponding instantaneous AoI. Note that the age gain of a device depends on only its instantaneous AoI under the *generate-at-will* (GAW) arrival of updates.

With this objective, scheduling schemes that operate in a centralized manner have been designed to perform close to optimal network AAoI in various scenarios [5]–[8]. However, they may be impractical due to the huge overhead of required coordination, especially when there is considerable uncertainty on the arrival patterns of updates. Unlike scheduling schemes, random access schemes (e.g. slotted ALOHA, frame slotted ALOHA, CSMA) allow a population of devices with limited or no coordination to dynamically and opportunistically share a channel. So, it is strongly required to design *age-gain-dependent random access* (AGDRA) schemes, where each device utilizes its knowledge of age gains[1] to determine when to transmit in an easily implementable decentralized manner, so that the unavoided contention can be limited to devices with age gains as high as possible.

Various AGDRA schemes have been proposed for the GAW arrival [10]–[17] and the Bernoulli arrival [18]–[21] of updates, and have been shown to significantly reduce the network AAoI compared to conventional random access schemes. It can be observed from [10]–[21] that designing AGDRA is uniquely challenging due to the inherent coupling of the arrival process of updates, the time evolution of local ages, the time evolution of AoIs, and the time-varying mutual interference. Generally speaking, this coupling would become more complicated when a more general arrival process of updates is considered, and is quite different from that for optimizing the throughput or delay metric.

B. Related Work

Without relying on the knowledge of age gains, many conventional random access schemes have been proposed for

This work was supported in part by the National Natural Science Foundation of China under Grant 62071236 and in part by the National Science and Technology Council, Taiwan, under Grant 112-2115-M-153-004-MY2. (*Corresponding author: Yijin Zhang*.)

Y. Zhu, Y. Zhu, Y. Lin, and Y. Zhang are with the School of Electronic and Optical Engineering, Nanjing University of Science and Technology, Nanjing 210094, China (e-mail: {yuqing.zhu; zyw; yanlin}@njust.edu.cn; yijin.zhang@gmail.com).

A. Gong is with the School of Computer and Communication Sciences, École Polytechnique Fédérale de Lausanne, Lausanne 1015, Switzerland (e-mail: aoyu.gong@epfl.ch).

Y.-H. Lo is with the Department of Applied Mathematics, National Pingtung University, Pingtung 90003, Taiwan (e-mail: yhlo@mail.nptu.edu.tw).

[1] In the language of decision making under uncertainty [9], a knowledge of age gains is defined as a probability distribution for the age gains of all the devices based on past decisions, past observations, and an estimation approach.

minimizing the network AAoI. Under the GAW arrival, [22] showed that using slotted ALOHA is worse than scheduling by a factor of about $2e$. Under the Bernoulli arrival, [23] used the elementary renewal theorem to optimize the transmission probabilities for slotted ALOHA and CSMA, while [24] used *discrete-time Markov chains* (DTMCs) to optimize the frame length for frame slotted ALOHA. Under the periodic arrival, [25] analyzed the effect of maximizing the instantaneous throughput on the network AAoI of slotted ALOHA.

Basic AGDRA, where each device utilizes its knowledge of age gain of only itself to adjust its access parameters, has been investigated in [10]–[16], [18], [21]. In the form of slotted ALOHA, [10]–[16] assumed that each device adopts a fixed transmission probability if its corresponding age gain reaches a fixed threshold, but keeps silent otherwise. Based on a comprehensive steady-state analysis of the DTMC defined in [10], closed-form expressions of the network AAoI and optimal access parameters were provided in [11] for an infinitely large network size. For an arbitrary network size, [12] analyzed the network AAoI by modeling the AoI evolution of each device as a DTMC, which, however, relies on an ideal assumption that the states of all the devices are independent of each other. To mitigate the negative impact of contentions, a reservation phase ahead of actual data transmission is proposed in [13], [14], but its benefit comes at the cost of additional overhead compared to [10]–[12]. Further, [15], [16] used stochastic geometry tools to derive the network AAoI under the spatiotemporal interference. Note that [10]–[16] mainly focused on the GAW traffic, except that [11] extended its findings to obtain an upper bound on the network AAoI for the Bernoulli arrival. These schemes [10]–[16] have a common advantage that the access parameters can be obtained offline through analytical modeling, and thus can be simply implemented. In addition, heuristic methods proposed in [18], [21] allow each device to use different transmission probabilities for different cases, but lack analytical modeling.

To further reduce the network AAoI, enhanced AGDRA, where each device utilizes its knowledge of age gains of all the devices to adjust its access parameters, has been investigated in [19], [20] for the Bernoulli arrival. In the form of slotted ALOHA, the AAT proposed in [19] allows each device to transmit with a dynamic transmission probability (determined by the estimated number of active devices) for maximizing the instantaneous network throughput only if its corresponding age gain reaches a threshold, which could be computed adaptively using the estimated distribution of age gains. In the form of frame slotted ALOHA, the T-DFSA proposed in [20] allows the frame length and age-gain threshold for each frame to be adjusted by the estimated distribution of age gains, so that the estimated expected number of active devices can be the smallest number not smaller than a certain number (searched by simulations). Different from [19], [20], under the GAW arrival, [17] estimated the network AoI rather than the individual age gains for heuristically adjusting the transmission probability, which would obviously lead to the AoI degradation.

However, these previous studies on AGDRA [10]–[21] have not considered the event-driven periodic arrival of updates, which usually appears in many monitoring services [26]–[28]. For example, in closed-loop process control, multiple sensors are employed to measure the plant outputs and validate the event conditions periodically, and then each sensor sends a fresh status update to a machine controller as needed. Note that such an arrival process can include GAW, Bernoulli, and periodic arrival processes considered in [10]–[25] as particular cases, and its primary technical difficulty is to deal with time-varying statistical characteristics of stochastic arrivals. [10]–[15], [18], [21] used steady-state analysis for either GAW or Bernoulli arrival processes; thus their models cannot be applied to analyze the transient behavior within each period. [25] used non-stationary analysis to study the transient behavior under periodic arrival but assumed a delivery deadline without setting an age gain threshold; thus lacked a characterization of the mutual effect of different periods on the age gains.

C. Contributions

To fill the gap in this field, this paper attempts to design a type of AGDRA in the form of slotted ALOHA with an age gain threshold [10]–[16], [19], [20], called T-AGDSA, under event-driven periodic updating. Compared to the existing work [11], [12], [19], [20], [25], this paper makes the following key contributions.

(i) Basic T-AGDSA: For simple implementation, consider fixed threshold and fixed transmission probability as in [10]–[16]. We provide an analytical modeling approach to evaluate the network AAoI under event-driven periodic updating, based on which optimal fixed threshold and optimal fixed transmission probability can be obtained offline. Compared to [11], [12], [25], the technical difficulty of our work is to consider the mutual impact of event-driven periodic updating and the age-gain-dependent behavior in modeling, which is overcome by a multi-layer DTMC model. Here an external DTMC manages the jumps between the beginnings of frames, while an internal DTMC manages the evolution during an arbitrary frame. Note that the modeling approaches in [12], [25] can be seen as special cases here.

(ii) Enhanced T-AGDSA: To pursue lower network AAoI, we propose an enhanced T-AGDSA scheme that allows each device to adjust the threshold and the transmission probability for maximizing the estimated network *expected AoI reduction* (EAR) per slot, based on the knowledge of age gains of all the devices. Our approach for acquiring such knowledge relies on using Bayes' rule to keep the a posteriori joint probability distribution for the local age and age gain of an arbitrary device given all of the globally available information. Compared with the AAT [19] that maximizes the estimated instantaneous network throughput under a reasonably controlled effective sum arrival rate, our scheme can avoid low efficiency of the throughput-EAR conversion. Compared with the T-DFSA [20] that controls the estimated expected number of active devices reasonably, our scheme can avoid the network EAR degradation when the probability distribution of the estimated number is divergent. Through extensive numerical experiments, we validate our theoretical analysis and demonstrate the advantage of the proposed schemes over the schemes in [11], [19], [20], [25] in a wide range of network configurations.

TABLE I
COMPARISON OF AGDRA SCHEMES.

Scheme	Traffic pattern	Access parameters	Required observations	Consider the dependence between age gains and local ages in modeling?	Rule of updating the knowledge of age gains
TA [11], ADRA [12]	GAW	Fixed	N/A	N/A	N/A
Basic T-AGDSA (Section III)	Event-driven periodic	Fixed	N/A	✓	N/A
AAT [19]	Bernoulli	Adaptive	Collision feedback	×	Bayesian rule
T-DFSA [20]	Bernoulli	Adaptive	Number of suc., idle, and colli. slots and the age gains of the successful devices	×	Maximum likelihood estimation
Enhanced T-AGDSA (Section IV)	Event-driven periodic	Adaptive	Channel status (idle/suc./colli.)	✓	Bayesian rule

The remainder of this paper is organized as follows. The system model, the considered two versions of T-AGDSA, and a lower bound on the network AAoI are specified in Section II. In Section III, we provide an analytical modeling approach to evaluate basic T-AGDSA for determining optimal fixed access parameters. In Section IV, we propose an enhanced T-AGDSA scheme for maximizing the estimated network EAR per slot. Section V provides numerical results to verify our study. Section VI draws final conclusions.

II. SYSTEM MODEL AND PRELIMINARIES

A. Network Model

Consider a globally-synchronized uplink IoT system consisting of a common *access point* (AP) and N devices, indexed by $\mathcal{N} \triangleq \{1, 2, ..., N\}$. The global channel time is divided into frames (indexed from frame 0), each of which consists of D consecutive slots, where $D \in \mathbb{Z}^+$ denotes the minimum update interval of each device. The slots in frame $m \in \mathbb{N}$ are indexed from slot mD to $(m+1)D-1$. At the beginning of each frame, each device independently generates a single-slot update with probability $\lambda \in (0, 1]$ and does not generate updates at other time points.[2] To maintain the information freshness, a newly generated update at each device will replace the undelivered older one if there is any.

By considering a reliable wireless channel under an appropriate modulation and coding scheme, we assume that an update is successfully transmitted if it is not involved in a collision, and otherwise is unsuccessfully transmitted. After a successful reception of an update of a device, the AP immediately sends an *acknowledgment* (ACK) to notify the device without errors or delays.[3] Thus, at the end of each slot t, each device is able to be aware of the channel status of slot t, denoted by $c_t \in \{0(\text{idle}), 1(\text{success}), *(\text{collision})\}$.

B. Performance Metrics

At the beginning of slot t, we denote the local age, proposed in [4], of device n by $w_{n,t}$, which measures the number of slots elapsed since the generation moment of its freshest update. The local age of device n is reset to zero if the device generates an update at the beginning of slot t, otherwise, it increases by one. Then, the evolution of $w_{n,t}$ with $w_{n,0} = 0$ is given by

$$w_{n,t+1} = \begin{cases} 0, & \text{if device } n \text{ generates an update} \\ & \text{at the beginning of slot } t+1, \\ w_{n,t} + 1, & \text{otherwise.} \end{cases} \quad (1)$$

Next, we denote the instantaneous AoI, proposed in [4], of device n at the beginning of slot t by $h_{n,t}$, which measures the number of slots elapsed since the generation moment of its most recently successfully transmitted update. If the freshest update of device n is transmitted successfully at slot t, the AoI of device n will be set to its local age (in the previous slot) plus one, otherwise, the AoI will increase by one. Then, the evolution of $h_{n,t}$ with $h_{n,0} = 0$ is given by

$$h_{n,t+1} = \begin{cases} w_{n,t} + 1, & \text{if device } n \text{ successfully} \\ & \text{transmits in slot } t, \\ h_{n,t} + 1, & \text{otherwise.} \end{cases} \quad (2)$$

Owing to the ACK mechanism and local information about $w_{n,t}$, each device n is able to be aware of the value of $h_{n,t+1}$ at the beginning of slot $t+1$ for each $t \geq 0$.

We define the AAoI of device n as:

$$\Delta_n \triangleq \lim_{T\to\infty} \frac{1}{T} \sum_{t=0}^{T-1} h_{n,t}, \quad (3)$$

where T is the time horizon length. We aim to design a random access protocol that minimizes the network AAoI,

$$\Delta \triangleq \frac{1}{N} \sum_{n=1}^{N} \Delta_n. \quad (4)$$

C. Random Access Protocol

We define the age gain, proposed in [29], of device n at the beginning of slot t as

$$g_{n,t} \triangleq h_{n,t} - w_{n,t}, \quad (5)$$

which quantifies the reduction in instantaneous AoI upon a successful transmission of device n. Based on the fact that $h_{n,t} \geq w_{n,t}$, it is clear that $g_{n,t} \geq 0$.

Following [19], we require each device n with a non-empty buffer (i.e., $g_{n,t} \geq 1$) to send its update according to the following T-AGDSA protocol, that is,

(i) transmits at the beginning of slot t with the probability $p_t \in (0, 1]$ if $g_{n,t} \geq \Gamma_t$, where $\Gamma_t \in \mathbb{Z}^+$ denotes the age gain threshold in slot t,

[2]This assumption holds when the devices with globally synchronized clocks validate the event conditions synchronously and periodically (e.g. in a periodic event-triggered control implementation for closed-loop process control [26]).
[3]This assumption holds when ACKs are well protected by error correction codes and the ACK length is negligible compared with the update length [10].

(ii) otherwise keeps silent at slot t.

A device n is said to be active in slot t if $g_{n,t} \geq \Gamma_t$.

Then, we consider the following two versions of T-AGDSA with different settings of Γ_t and p_t.

(i) Basic T-AGDSA: for simple implementation [11], the values of Γ_t and p_t are fixed to Γ^{sta} and p^{sta}, respectively, for all slots t.

(ii) Enhanced T-AGDSA: at the beginning of each slot t, each device utilizes the globally available information, including the network parameters N, λ, D, previous channel status c_{t-1}, and previous access parameters Γ_{t-1}, p_{t-1} to update the joint probability distribution of local age and age gain of an arbitrary device in a Bayesian manner, and uses this distribution to obtain the knowledge of age gains. Note that, similar to [19], since the devices only use globally available information to compute Γ_t, p_t individually, each device would obtain the same knowledge of age gains and compute the same values of Γ_t, p_t, without the need of sharing.

It will be shown in Sections III–V that basic T-AGDSA can be developed offline through theoretical modeling and is simpler to implement online compared to enhanced T-AGDSA, but *cannot* utilize the knowledge of age gains to improve the AoI performance as done in enhanced T-AGDSA.

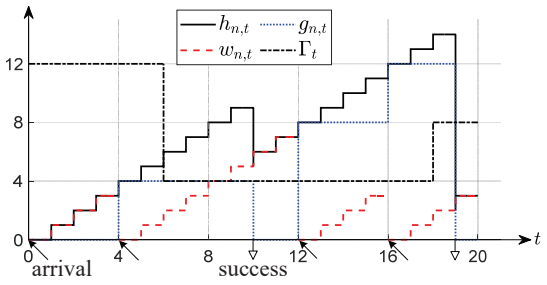

Fig. 1. An example of $h_{n,t}$, $w_{n,t}$, $g_{n,t}$ and Γ_t evolving over time under enhanced T-AGDSA when $D = 4$. The black solid arrowhead indicates the arrival of an update, whereas the black hollow arrowhead indicates the successful transmission of the most recently generated update of device n in the corresponding slot.

An example of $h_{n,t}$, $w_{n,t}$, $g_{n,t}$ and Γ_t evolving over time under enhanced T-AGDSA when $D = 4$ is shown in Fig. 1.

D. Lower bound

When $D = 1$, [19] derived a lower bound on the achievable network AAoI by assuming that all updates can be delivered instantaneously upon their arrival, without experiencing collisions. We extend this bound to the case $D \geq 1$. This bound is tighter when $N\lambda/D$ is smaller, which will be verified in Section V. The proof is given in the Appendix.

Proposition 1: For any transmission scheme under the system model specified in Section II-A,

$$\Delta \geq D/\lambda + (1 - D)/2. \tag{6}$$

III. Modeling and Design of Basic T-AGDSA

In this section, we provide an analytical modeling approach to evaluate the network AAoI of basic T-AGDSA, and use this modeling to obtain optimal values of fixed threshold Γ^{sta} and fixed transmission probability p^{sta}.

The symmetric scenario described in Section II allows us to analyze the AAoI of an arbitrarily tagged device to represent the network AAoI. So, we omit the device index for analysis simplicity. To reflect the impact of the frame length D better, we identify a slot t by the tuple (m, ν), where $m = \lfloor t/D \rfloor$ and $\nu = t - mD$, for arbitrary $t \geq 0$.

To deal with the mutual effect of different frames and the transient behavior within each frame, which are over different time scales, we decompose the system in two nested layers (as shown in Fig. 2) using a multi-layer Markov model where the external layer manages the jumps between consecutive beginnings of frames, while the internal layer manages the evolution during an arbitrary frame. In the rest of this section, we explore how to establish these two layers.

A. External Layer

Let W_m and H_m denote the local age and instantaneous AoI of the tagged device at the beginning of frame m, respectively. By Eq. (1) and the traffic pattern described in Section II, the evolution of W_m with $W_0 = 0$ can be expressed as

$$W_{m+1} = \begin{cases} 0, & \text{if an update arrives at the} \\ & \text{beginning of frame } m+1, \\ W_m + D, & \text{otherwise.} \end{cases} \tag{7}$$

By Eq. (2), the evolution of H_m with $H_0 = 0$ is

$$H_{m+1} = \begin{cases} W_m + D, & \text{if an update is successfully} \\ & \text{transmitted during frame } m, \\ H_m + D, & \text{otherwise.} \end{cases} \tag{8}$$

Denote the age gain of the tagged device at the beginning of frame m by G_m. By Eq. (5), we have

$$G_m = H_m - W_m. \tag{9}$$

Consider a state process $\boldsymbol{X} \triangleq \{X_m, m \in \mathbb{N}\}$ where $X_m \triangleq (W_m, G_m)$. By Eqs. (7)–(9), we observe that the transition to the next state in $\boldsymbol{X}$ depends only on the present state and not on the previous states. Hence, $\boldsymbol{X}$ can be viewed as a DTMC with the infinite state space $\mathcal{X} \triangleq \{(lD, kD) | l, k \in \mathbb{N}\}$.

For an arbitrary frame m with $X_m = (lD, kD)$, let $\alpha_{l,k,\nu}$ and $\beta_{l,k}$ denote the probabilities that the tagged device transmits its update successfully at slot (m, ν) and in frame m, respectively. Obviously, $\beta_{l,k} = \sum_{\nu=0}^{D-1} \alpha_{l,k,\nu}$. According to the evolution of W_m and G_m given in Eqs. (7)–(9), the state transition probabilities of $\boldsymbol{X}$ can be obtained as

$$\begin{aligned} &P^{\boldsymbol{X}}_{(lD,kD),(l'D,k'D)} \\ &\triangleq \Pr\big(X_{m+1} = (l'D, k'D) \mid X_m = (lD, kD)\big) \\ &= \begin{cases} \lambda\beta_{l,k}, & \text{if } l' = 0, k' = l+1, \\ \lambda(1-\beta_{l,k}), & \text{if } l' = 0, k' = l+k+1, \\ (1-\lambda)\beta_{l,k}, & \text{if } l' = l+1, k' = 0, \\ (1-\lambda)(1-\beta_{l,k}), & \text{if } l' = l+1, k' = k, \\ 0, & \text{otherwise.} \end{cases} \end{aligned} \tag{10}$$

Consider that under the traffic pattern described in Section II, the age gain of the tagged device during frame m remains unchanged if the tagged device fails to transmit its

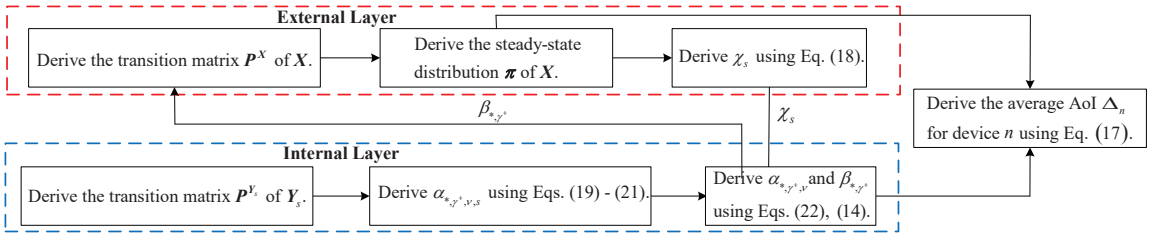

Fig. 2. Flowchart illustrating the basic idea of analyzing basic T-AGDSA.

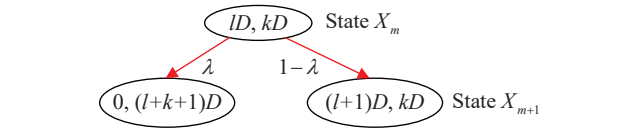

(a) $l \geq 0, 0 \leq k \leq \gamma - 1$.

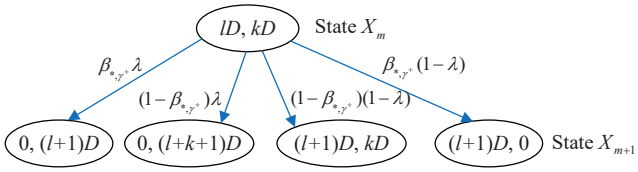

(b) $l \geq 0, k \geq \gamma$.

Fig. 3. The external DTMC $\boldsymbol{X}$.

update successfully in frame m; otherwise, the age gain will reduce to zero and remain zero in the subsequent slots during frame m after a successful transmission. Thus, the age gain of the tagged device in each slot takes value from $\{0, D, 2D, \ldots\}$. This observation allows us to set $\gamma \triangleq \lceil \Gamma^{\text{sta}}/D \rceil$, and discuss possible values of $\alpha_{l,k,\nu}$ and $\beta_{l,k}$ in Eq. (10) based on different values of l, k, ν and γ.

Case 1: When $l \geq 0, 0 \leq k \leq \gamma - 1$, we have $G_m \leq (\gamma - 1)D < \Gamma^{\text{sta}}$. Consider that the tagged device keeps its age gain unchanged during frame m if it does not make a successful transmission during frame m. So, the tagged device always keeps silent in frame m as its age gain is always smaller than Γ^{sta}. Then we obtain

$$\alpha_{l,k,\nu} = 0, \tag{11}$$

$$\beta_{l,k} = \sum_{\nu=0}^{D-1} \alpha_{l,k,\nu} = 0, \tag{12}$$

if $l \geq 0, 0 \leq k \leq \gamma - 1$, $0 \leq \nu \leq D - 1$. With Eqs. (10)–(12), the state transitions for this case are illustrated in Fig. 3(a).

Case 2: When $l \geq 0, k \geq \gamma$, we have $G_m \geq \gamma D \geq \Gamma^{\text{sta}}$, the tagged device transmits its update with a fixed probability p^{sta} at the beginning of slot (m, ν) when $0 \leq \nu \leq D - 1$ until a successful transmission. Note that the tagged device behaves the same during frame m regardless of the values of W_m, G_m when $G_m \geq \gamma D$. So, we rewrite $\alpha_{l,k,\nu}$ and $\beta_{l,k}$ simply as

$$\alpha_{l,k,\nu} = \alpha_{*,\gamma^+,\nu}, \tag{13}$$

$$\beta_{l,k} = \sum_{\nu=0}^{D-1} \alpha_{*,\gamma^+,\nu} = \beta_{*,\gamma^+}, \tag{14}$$

if $l \geq 0, k \geq \gamma$, $0 \leq \nu \leq D - 1$. Both $\alpha_{*,\gamma^+,\nu}$ and β_{*,γ^+} are independent of values of l and k. With Eqs. (10), (13), and (14), the state transitions for this case is illustrated in Fig. 3(b).

Note that the state $(0, 0)$ in $\boldsymbol{X}$ is an ephemeral state only occurring when $m = 0$ (i.e., $t = 0$), while the remaining states are all in the same recurrent class and occur when $m \geq 1$ (i.e., $t \geq D$). As m increases, $\boldsymbol{X}$ will get absorbed in the recurrent class and stay there forever. Denote by $\boldsymbol{\pi} \triangleq (\pi_{lD,kD})_{l,k \in \mathbb{N}}$ the steady-state distribution of $\boldsymbol{X}$. Each element $\pi_{lD,kD}$ denotes the steady-state probability of $\boldsymbol{X}$ staying at state (lD, kD). We assume that $\pi_{0,0} = 0$.

Then, for different states in $\boldsymbol{X}$, we consider the following two cases for evaluating the AAoI of the tagged device during an arbitrary frame m with $X_m = (lD, kD)$.

Case 1: The tagged device transmits its update successfully at slot (m, ν) given $X_m = (lD, kD)$. Let $\Delta_{l,k,\nu}$ denote the AAoI of the tagged device during frame m when this event occurs. We have

$$\begin{aligned}\Delta_{l,k,\nu} &= \frac{1}{D}\Big(\sum_{\nu'=0}^{\nu} \big((l+k)D + \nu'\big) + \sum_{\nu'=\nu+1}^{D-1} (lD + \nu') \Big) \\ &= lD + k(\nu+1) + \frac{D-1}{2}. \end{aligned} \tag{15}$$

Case 2: The tagged device fails to transmit its update successfully during frame m given $X_m = (lD, kD)$. Let $\Delta_{l,k,*}$ denote the AAoI of the tagged device during frame m when this event occurs. We have

$$\Delta_{l,k,*} = \frac{\sum_{\nu=0}^{D-1} \big((l+k)D + \nu\big)}{D} = (l+k)D + \frac{D-1}{2}. \tag{16}$$

Based on the DTMC $\boldsymbol{X}$ and Eqs. (15), (16), the AAoI of an arbitrary device n can be derived as

$$\begin{aligned}\Delta_n &= \sum_{l=0}^{\infty}\sum_{k=0}^{\infty} \pi_{lD,kD} \Big(\sum_{\nu=0}^{D-1} \alpha_{l,k,\nu}\Delta_{l,k,\nu} + (1-\beta_{l,k})\Delta_{l,k,*} \Big) \\ &= \sum_{l=0}^{\infty}\sum_{k=\gamma}^{\infty} \pi_{lD,kD} \Big(\sum_{\nu=0}^{D-1} \alpha_{*,\gamma^+,\nu}\Delta_{l,k,\nu} + (1-\beta_{*,\gamma^+})\Delta_{l,k,*} \Big) \\ &\quad + \sum_{l=0}^{\infty}\sum_{k=0}^{\gamma-1} \pi_{lD,kD}\Delta_{l,k,*}. \end{aligned} \tag{17}$$

In the following, we will derive $\alpha_{*,\gamma^+,\nu}$, which is necessary to compute Δ_n based on Eqs. (15)–(17).

B. Internal Layer to Evaluate $\alpha_{*,\gamma^+,\nu}$

Note that whether the tagged device can transmit its update successfully depends on the behaviors of all active devices during frame m. Let a random variable S_m denote the number of active devices not including the tagged device at the beginning of an arbitrary frame m, and let χ_s denote the probability mass function of $S_m = s$. Following [12], we make a simplifying decoupling assumption that the states of all the devices are independent of each other. Then, based on the binomial distribution, for each $0 \le s \le N-1$, we have

$$\chi_s = \binom{N-1}{s} \Big(\sum_{l=0}^{\infty} \sum_{k=\gamma}^{\infty} \pi_{lD,kD} \Big)^s \Big(\sum_{l=0}^{\infty} \sum_{k=0}^{\gamma-1} \pi_{lD,kD} \Big)^{N-1-s}. \tag{18}$$

Consider an arbitrary frame m with $G_m \ge \gamma D$ and $S_m = s$. Define $\boldsymbol{Y}_s \triangleq \{Y_{s,\nu}, \nu = 0, 1, \ldots, D\}$ as an absorbing DTMC with the finite state space $\mathcal{Y}_s \triangleq \{0, 1, \ldots, s, suc\}$, as shown in Fig. 4. The states $Y_{s,\nu} = y$ with $0 \le \nu \le D, 0 \le y \le s$ are transient states indicating that, during frame m, the tagged device has not transmitted successfully before the beginning of slot (m, ν) while other y devices have transmitted successfully before the beginning of slot (m, ν). The state $Y_{s,\nu} = suc$ is an absorbing state indicating that, during frame m, the tagged device has transmitted successfully before the beginning of slot (m, ν). For convenience, the slot index (m, D) is used to denote the slot index $(m+1, 0)$ here. As shown in Fig. 4, the state transition probabilities of $\boldsymbol{Y}_s$ can be obtained as

$$P_{y,y'}^{\boldsymbol{Y}_s} \triangleq \Pr\big(Y_{s,\nu+1} = y' \mid Y_{s,\nu} = y\big) = \begin{cases} 1-(s-y+1)p^{\text{sta}}(1-p^{\text{sta}})^{s-y}, & \\ \qquad\qquad \text{if } 0 \le y \le s, y' = y, & \\ (s-y)p^{\text{sta}}(1-p^{\text{sta}})^{s-y}, & \\ \qquad\qquad \text{if } 0 \le y \le s-1, y' = y+1, & \\ p^{\text{sta}}(1-p^{\text{sta}})^{s-y}, \quad \text{if } 0 \le y \le s, y' = suc, & \\ 1, \qquad\qquad \text{if } y = y' = suc, & \\ 0, \qquad\qquad \text{otherwise.} & \end{cases} \tag{19}$$

The first case in Eq. (19) corresponds to that no device transmits successfully in slot (m, ν) when $0 \le y \le s$. The second case corresponds to that one of the other $(s-y)$ devices transmits successfully in slot (m, ν) when $0 \le y \le s-1$. The third case corresponds to that the tagged device transmits successfully in slot (m, ν) when $0 \le y \le s$. The fourth case corresponds to that the tagged device has made a successful transmission before the beginning of slot (m, ν).

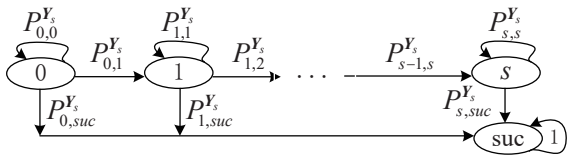

Fig. 4. The internal absorbing DTMC $\boldsymbol{Y}$.

Let $\boldsymbol{\varphi}_{s,\nu}$ denote the state vector of $Y_{s,\nu}$, where the i-th element corresponds to the state $i-1$ for $1 \le i \le s+1$ and the last element corresponds to the state suc. Then, given the priori state vector $\boldsymbol{\varphi}_{s,0} \triangleq [1, 0, 0, \ldots, 0]$ and the transition matrix $\boldsymbol{P}^{\boldsymbol{Y}_s}$ based on Eq. (19), by applying a simple power method, for each $0 \le \nu \le D$ and $0 \le s \le N-1$, we have

$$\boldsymbol{\varphi}_{s,\nu} = \boldsymbol{\varphi}_{s,0} (\boldsymbol{P}^{\boldsymbol{Y}_s})^{\nu}. \tag{20}$$

Let $\alpha_{*,\gamma^+,\nu,s}$ denote the probability that the tagged device transmits successfully in slot (m, ν) of an arbitrary frame m with $G_m \ge \gamma D$, $S_m = s$. Then, we have

$$\alpha_{*,\gamma^+,\nu,s} = \boldsymbol{\varphi}_{s,\nu+1}(s+2) - \boldsymbol{\varphi}_{s,\nu}(s+2), \tag{21}$$

for each $0 \le \nu \le D-1$ and $0 \le s \le N-1$. By Eqs. (18) and (21), for each $0 \le \nu \le D-1$, we have

$$\alpha_{*,\gamma^+,\nu} = \sum_{s=0}^{N-1} \chi_s \alpha_{*,\gamma^+,\nu,s}. \tag{22}$$

C. Evaluation of Δ_n

Now we are ready to use the following three steps to compute Δ_n by connecting the external and internal layers proposed in previous subsections.

Step 1: Based on the transition probabilities in Eq. (10), the steady-state distribution $\boldsymbol{\pi}$ can be obtained by solving a set of linear equations

$$\boldsymbol{\pi} \boldsymbol{P}^{\boldsymbol{X}} = \boldsymbol{\pi}, \tag{23}$$

and the normalizing condition

$$\sum_{l=0}^{\infty} \sum_{k=0}^{\infty} \pi_{lD,kD} = 1. \tag{24}$$

Since β_{*,γ^+} is involved as the only unknown parameter in the transition matrix $\boldsymbol{P}^{\boldsymbol{X}}$, each $\pi_{lD,kD}$ can be expressed as a function of β_{*,γ^+} using a mathematical induction method based on Eqs. (10), (23), (24). Meanwhile, $\alpha_{*,\gamma^+,\nu}$ in Eq. (14) can be expressed as a function of $\pi_{lD,kD}, l, k \in \mathbb{N}$ based on Eqs. (18)–(22). Hence, we can obtain the value of β_{*,γ^+} by solving Eq. (14) using numerical methods.

Step 2: With the value of β_{*,γ^+}, we can obtain the values of $\pi_{lD,kD}, l, k \in \mathbb{N}$ since each $\pi_{lD,kD}$ can be expressed as a function of β_{*,γ^+}, and then obtain the values of $\alpha_{*,\gamma^+,\nu}, 0 \le \nu \le D-1$ by Eqs. (18)–(22).

Step 3: With the values of $\pi_{lD,kD}, l, k \in \mathbb{N}$, $\alpha_{*,\gamma^+,\nu}, 0 \le \nu \le D-1$ and β_{*,γ^+}, we can obtain the AAoI for an arbitrary device n by Eq. (17).

Remark 1: When $\Gamma^{\text{sta}} = \lambda = 1$, we note that we can drop the subscripts l, k of $\beta_{l,k}$ and have $\pi_{0,kD} = \beta(1-\beta)^{k-1}$ for $k \ge 1$ since $\beta_{l,k}$ is independent of l and k. So, our modeling approach is reduced to that in [25].

Remark 2: When $D = \lambda = 1$ (i.e., the GAW traffic), we have $W_m = 0$, $H_m = G_m$ for each $m \in \mathbb{N}$, and

$$\beta_{*,\gamma} = \beta_{*,\gamma^+} = \alpha_{*,\gamma,0} = \alpha_{*,\gamma^+,0} = \sum_{s=0}^{N-1} \chi_s p^{\text{sta}} (1-p^{\text{sta}})^s = p^{\text{sta}} (1 - p^{\text{sta}} \sum_{k=\gamma}^{\infty} \pi_{0,k})^{N-1}. \tag{25}$$

So, our modeling approach is reduced to that in [12].

Remark 3: When $D = \lambda = 1$, [11] presented a precise steady-state analysis without assuming that the states of all the devices are independent of each other. A key idea therein is to utilize an inherent feature for $D = \lambda = 1$, that is, different inactive devices have different age gains. However, it is inapplicable for $D > 1$ or $\lambda < 1$ because there may exist multiple inactive devices with the same age gain.

D. Seeking Optimal Γ^{sta} and p^{sta}

To seek optimal values of Γ^{sta} and p^{sta}, we can view Δ_n given in Eq. (17) as a function of both Γ^{sta} and p^{sta}, denoted by $\Delta_n(\Gamma^{\text{sta}}, p^{\text{sta}})$. However, it is difficult to obtain the gradient of $\Delta_n(\Gamma^{\text{sta}}, p^{\text{sta}})$ due to the lack of an explicit expression. So, gradient-free search methods need to be applied. Since the age gain of each device is always an integral multiple of D as described in Section III-A, we can consider only $\Gamma^{\text{sta}} = kD, k = 1, 2, \ldots$ to reduce the search space.

E. Impacts of Network Parameters

By Eqs. (14), (18)–(22), we know both $\alpha_{*,\gamma^+,\nu}$, β_{*,γ^+} decrease with N since the value range of s grows with N, which leads to an increment of the term $\sum_{\nu=0}^{D-1} \alpha_{*,\gamma^+,\nu}\Delta_{l,k,\nu} + (1 - \beta_{*,\gamma^+})\Delta_{l,k,*}$ in Eq. (17). In addition, as β_{*,γ^+} decreases, the steady-state probabilities $\pi_{lD,kD}$ become larger for large k, which also leads to an increment of Eq. (17). These impacts are verified by Fig. 6, which shows that the network AAoI always increases with N.

By Eq. (10) and Fig. 3, we observe that $(\pi_{0,kD})_{k\in\mathbb{N}}$ increases with λ, which leads to a reduction of Eq. (17). Obviously, the age gains of all the devices tend to change to larger values more frequently as λ increases. By this observation and Eqs. (14), (18)–(22), we know that both $\alpha_{*,\gamma^+,\nu}$ and β_{*,γ^+} decrease with λ, which leads to an increment of Eq. (17). By Eqs. (10), (14), (18)–(22), we further know this increment would become larger as N increases, λ increase or D decreases. These impacts are verified by Fig. 6, which shows that the network AAoI decreases with λ, and the decreasing trend becomes gentler as N increases, λ increases or D decreases.

By Eqs. (15), (16), we know that the terms $\Delta_{l,k,\nu}$ and $\Delta_{l,k,*}$ in Eq. (17) both increase linearly with D. By Eqs. (14), (18)–(22), we know that β_{*,γ^+} increases with D, leading to a decrement of the term $(1 - \beta_{*,\gamma^+})$ in Eq. (17). Further, by Eq. (10) and Fig. (3), we know that $\pi_{lD,kD}$ would become larger for small k as β_{*,γ^+} increases, which also leads to a decrement of Eq. (17). By Eqs. (10), (14), (18)–(22), we further know these two decrements would become larger as N increases, λ increases or D decreases. These impacts are verified by Fig. 6, which shows that the network AAoI increases with D, and the increasing trend gradually becomes gentle as N increases, λ increases or D decreases.

F. Complexity analysis

Following [19], [20], we set a large integer U to truncate the maximum values of local ages and age gains for practical implementation. The basic T-AGDSA has an online computational complexity $\mathcal{O}(1)$, but has an offline computational complexity $(C_{\text{numer}}+\mathcal{O}(\frac{U^2}{D^2}+N^2D+\frac{U^2}{D}))E_{\text{2search}}$ where C_{numer} denotes the complexity of the used numerical method for solving the single-variable function of β_{*,γ^+}, $\mathcal{O}(\frac{U^2}{D^2} + N^2D)$ is the complexity of computing Eqs. (18)–(22), $\mathcal{O}(\frac{U^2}{D})$ is the complexity of computing Eq. (17), and E_{2search} denotes the number of the evaluations for seeking optimal Γ^{sta}, p^{sta} under the used two-dimensional gradient-free search method. For example, the derivative-free nonmonotone line search method yields $C_{\text{numer}} \leq \mathcal{O}((\frac{U^2}{D^2} + N^2D)\frac{|\log\sigma|}{\sigma^2})$ [30] and the directional direct-search method yields $E_{\text{2search}} \leq \mathcal{O}(\frac{U}{D\epsilon^2})$ [31], where σ, ϵ both denote the solution accuracy.

IV. Design of Enhanced T-AGDSA

In this section, we propose an enhanced T-AGDSA scheme that allows each device to adjust the threshold Γ_t and the transmission probability p_t for maximizing the estimated network EAR per slot, based on the knowledge of age gains of all the devices. After introducing the basic idea of our design, we will present a comprehensive explanation of the three key steps as shown in Fig. 5.

A. Basic Idea

Define the AoI reduction of device n in slot t as

$$r_{n,t} \triangleq h_{n,t} - h_{n,t+1}. \tag{26}$$

We can use Eqs. (2), (5) and (26) to compute $r_{n,t}$ as follows.

$$r_{n,t} = \begin{cases} (w_{n,t}+g_{n,t})-(w_{n,t}+1) \\ = g_{n,t} - 1, & \text{if device } n \text{ successfully} \\ & \text{transmits in slot } t, \\ h_{n,t}-(h_{n,t}+1) = -1, & \text{otherwise.} \end{cases} \tag{27}$$

Let $\theta_{n,t}$ denote the success probability when device n transmits in slot t. From Eq. (27), we can obtain the EAR of device n in slot t as

$$\begin{aligned} R_{n,t} \triangleq \mathbb{E}(r_{n,t}) &= \big((g_{n,t} - 1)p_t\theta_{n,t} - (1 - p_t\theta_{n,t})\big)I_{g_{n,t}\geq\Gamma_t} \\ &\quad + (-1)I_{0\leq g_{n,t}<\Gamma_t} \\ &= \big(g_{n,t}p_t\theta_{n,t} - 1\big)I_{g_{n,t}\geq\Gamma_t} - I_{0\leq g_{n,t}<\Gamma_t} \\ &= -1 + g_{n,t}p_t\theta_{n,t}I_{g_{n,t}\geq\Gamma_t}, \\ &= -1 + g_{n,t}p_t(1 - p_t)^{u_{n,t}}I_{g_{n,t}\geq\Gamma_t}, \end{aligned} \tag{28}$$

where $\mathbb{E}(\cdot)$ denotes the expectation operator, I_ψ is the indicator function which equals 1 if the event ψ is true and 0 otherwise, and $u_{n,t} \triangleq \sum_{n'=1,n'\neq n}^{N} I_{g_{n',t}\geq\Gamma_t}$ denotes the number of active devices not including device n in slot t. Then, the network EAR in slot t can be obtained as

$$R_t \triangleq \frac{\sum_{n=1}^{N} R_{n,t}}{N}. \tag{29}$$

This section will investigate how each device uses globally available information to choose Γ_t and p_t for maximizing R_t. Note that, although it may be possible to achieve better results by using information local to the devices, or using a strategy to maximize the long-run network EAR that is not "one-step look-ahead", we do not pursue these possibilities here.

From Eqs. (28)–(29), we see that the values of the age gains $g_{n,t},\ n \in \mathcal{N}$ is essential for maximizing R_t. However, in practice, it is impossible for each device to obtain precise values of the age gains of other devices. So, to obtain a knowledge of age gains, we require each device to keep the a posteriori joint probability distribution of local age and age gain of an arbitrarily tagged device at the beginning of slot t, given all of the globally available information. We denote this distribution by $(\hat{f}_{t,w,g})_{w,g\in\mathbb{N}}$, where $\hat{f}_{t,w,g} \triangleq \Pr\big(w_{n,t} = w, g_{n,t} = g\big), w, g \in \mathbb{N}$. Based on $(\hat{f}_{t,w,g})_{w,g\in\mathbb{N}}$, a brief introduction of the three key steps of the proposed enhanced T-AGDSA as shown in Fig. 5 is given below:

Step 1: At the beginning of slot t, each device uses $(\hat{f}_{t,w,g})_{w,g\in\mathbb{N}}$ to obtain an estimate of network EAR, denoted by $\hat{R}_t$, and then chooses Γ_t and p_t that maximize $\hat{R}_t$.

Step 2: At the end of slot t, each device uses the observed channel status Γ_t, p_t, c_t to update $(\hat{f}_{t,w,g})_{w,g\in\mathbb{N}}$ in a Bayesian manner. We denote the resulting distribution in this step by $(\hat{f}_{t^+,w,g})_{w,g\in\mathbb{N}}$, where t^+ represents the end of slot t.

Step 3: At the beginning of slot $t+1$, if $t = mD-1, m \in \mathbb{Z}^+$, each device obtains $(\hat{f}_{t+1,w,g})_{w,g\in\mathbb{N}}$ using $(\hat{f}_{t^+,w,g})_{w,g\in\mathbb{N}}$ and the update generation probability λ, otherwise, each device obtains $(\hat{f}_{t+1,w,g})_{w,g\in\mathbb{N}} = (\hat{f}_{t^+,w,g})_{w,g\in\mathbb{N}}$.

Note that these steps are also related to how to update $(\hat{f}_{t,w,g})_{w,g\in\mathbb{N}}$. Obviously, as only globally available information is used in these steps, each device would obtain the same $(\hat{f}_{t,w,g})_{w,g\in\mathbb{N}}$, and thus obtain the same knowledge of age gains without the need of sharing.

Remark 4: In AAT [19], Γ_t is chosen so that the effective sum arrival rate approaches $1/e$ as close as possible and p_t is then chosen for maximizing the instantaneous network throughput. However, such a setting may yield unsatisfactory network EAR, since it allows the devices with low age gains to compete for the transmission opportunity as soon as the effective sum arrival rate does not exceed $1/e$. In other words, in a slot, higher network throughput *cannot* be certainly converted to larger network EAR.

Remark 5: In T-DFSA [20], the maximum value of the thresholds that make the estimated expected number of active devices not smaller than a certain number (searched by simulations) is chosen. However, such a setting may yield unsatisfactory network EAR, since its design objective may be far from maximizing the network EAR, especially when the probability distribution of the estimated number is divergent.

Remark 6: Both AAT [19] and T-DFSA [20] ideally assume that the age gain and local age of a device are independent of each other, thus only consider the distribution of age gain. However, there is a strong dependence between them as described in Eq. (5). This is indeed why we consider $(\hat{f}_{t,w,g})_{w,g\in\mathbb{N}}$.

Remark 7: The AAT [19] utilizes only the collision feedback to update its estimate, while our enhanced T-AGDSA scheme utilizes the ternary feedback (idle, success, collision). Nevertheless, our scheme requires no additional overhead owing to the ACK mechanism.

B. Choosing Γ_t and p_t based on $(\hat{f}_{t,w,g})_{w,g\in\mathbb{N}}$

In the following, we present how to estimate the network EAR in slot t based on $(\hat{f}_{t,w,g})_{w,g\in\mathbb{N}}$ by assuming that the states of all the devices are independent of each other.

Let $\hat{u}_t$ denote the estimated number of active devices not including an arbitrary device in slot t, and let $\xi_{t,u}$ denote the probability mass function of $\hat{u}_t = u$. Based on the binomial distribution, we have

$$\xi_{t,u} = \binom{N-1}{u} \rho_t^u (1-\rho_t)^{N-1-u}, \tag{30}$$

for each $0 \le u \le N-1$, where

$$\rho_t = \sum_{w=0}^{\infty} \sum_{g=\Gamma_t}^{\infty} \hat{f}_{t,w,g}, \tag{31}$$

denotes the probability of an arbitrary device being active in slot t.

From Eq. (30), we obtain the estimated success probability of an arbitrary transmission in slot t as follows.

$$\hat{\theta}_t = \sum_{u=0}^{N-1} \xi_{t,u} (1-p_t)^u. \tag{32}$$

From Eqs. (27) and (32), we can obtain the following estimate of network EAR in slot t.

$$\begin{aligned} \hat{R}_t &= \sum_{w=0}^{\infty} \sum_{g=0}^{\infty} \hat{f}_{t,w,g} \big(-1 + g p_t \hat{\theta}_t I_{g \ge \Gamma_t} \big) \\ &= -1 + \big(\sum_{w=0}^{\infty} \sum_{g=\Gamma_t}^{\infty} \hat{f}_{t,w,g} g \big) p_t \hat{\theta}_t \end{aligned} \tag{33}$$

We can view $\hat{R}_t$ as a function of Γ_t and p_t, denoted by $\hat{R}_t(\Gamma_t, p_t)$. We see from Eq. (33) that, for each given $\Gamma_t \ge 1$, the maximization of $\hat{R}_t(\Gamma_t, p_t)$ is equivalent to the maximization of $p_t \hat{\theta}_t$. So, we can obtain the value p_t^o that maximizes $p_t \hat{\theta}_t$ by differentiating and root finding since $p_t \hat{\theta}_t$ is a polynomial of p_t. However, in practice, such computation would probably be excessive. Following [32], [33], we can approximate p_t^o as follows.

$$\hat{p_t^o} = \min\{\frac{1}{N\rho_t}, 1\}. \tag{34}$$

C. Computing $(\hat{f}_{t^+,w,g})_{w,g\in\mathbb{N}}$ Using Channel Observations

Let w_{n,t^+} and g_{n,t^+} denote the local age and age gain of an arbitrary device n at the end of slot t, respectively. Given all globally available information at the end of slot t, each device is able to compute $\hat{f}_{t^+,w',g'}$ using Bayes' rule as follows.

$$\begin{aligned} &\hat{f}_{t^+,w',g'} \\ &\triangleq \Pr\big(w_{n,t^+} = w', g_{n,t^+} = g' | \Gamma_t, p_t, c_t = c, (\hat{f}_{t,w,g})_{w,g\in\mathbb{N}}\big) \\ &= \frac{1}{\rho} \sum_{w,g\in\mathbb{N}} \hat{f}_{t,w,g} \Pr\big(w_{n,t^+} = w', g_{n,t^+} = g', c_t = c | \Gamma_t, \\ &\qquad\qquad p_t, w_{n,t} = w, g_{n,t} = g\big), \end{aligned} \tag{35}$$

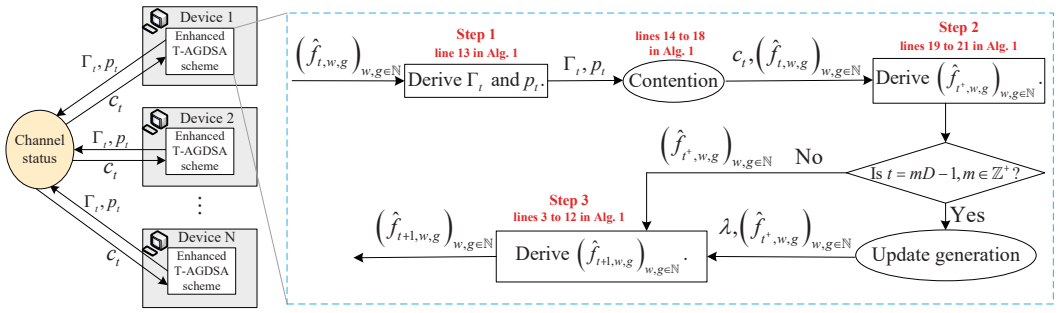

Fig. 5. Flowchart of the enhanced T-AGDSA illustrating the three main steps in Algorithm 1.

for each $t, w', g' \in \mathbb{N}$, where

$$\rho = \sum_{w'',g''\in\mathbb{N}} \sum_{w,g\in\mathbb{N}} \hat{f}_{t,w,g} \Pr\big(w_{n,t^+} = w'', g_{n,t^+} = g'', c_t = c | \Gamma_t, p_t, w_{n,t} = w, g_{n,t} = g\big), \tag{36}$$

$$\Pr\big(w_{n,t^+} = w', g_{n,t^+} = g', c_t = c | \Gamma_t, p_t, w_{n,t} = w, g_{n,t} = g\big) = \begin{cases} (1-p_t)\sum_{u=0}^{N-1} \xi_{t,u}(1-p_t)^u, \\ \quad \text{if } g \geq \Gamma_t, c = 0, w' = w+1, g' = g, \\ \sum_{u=0}^{N-1} \xi_{t,u}(1-p_t)^u, \\ \quad \text{if } 0 \leq g < \Gamma_t, c = 0, w' = w+1, g' = g, \\ (1-p_t)\sum_{u=1}^{N-1} \xi_{t,u} u p_t (1-p_t)^{u-1}, \\ \quad \text{if } g \geq \Gamma_t, c = 1, w' = w+1, g' = g, \\ \sum_{u=1}^{N-1} \xi_{t,u} u p_t (1-p_t)^{u-1}, \\ \quad \text{if } 0 \leq g < \Gamma_t, c = 1, w' = w+1, g' = g, \\ p_t \sum_{u=0}^{N-1} \xi_{t,u}(1-p_t)^u, \\ \quad \text{if } g \geq \Gamma_t, c = 1, w' = w+1, g' = 0, \\ \sum_{u=1}^{N-1} \xi_{t,u} \sum_{u'=2}^{u+1} \binom{u+1}{u'} p_t^{u'} (1-p_t)^{u+1-u'}, \\ \quad \text{if } g \geq \Gamma_t, c = *, w' = w+1, g' = g, \\ \sum_{u=2}^{N-1} \xi_{t,u} \sum_{u'=2}^{u} \binom{u}{u'} p_t^{u'} (1-p_t)^{u-u'}, \\ \quad \text{if } 0 \leq g < \Gamma_t, c = *, w' = w+1, g' = g, \\ 0, \quad \text{otherwise.} \end{cases} \tag{37}$$

In Eq. (37), the first and second cases correspond to that no devices transmit, the third and fourth cases correspond to that one of the other $N-1$ devices transmits successfully, the fifth case corresponds to that the tagged device transmits successfully when it is active in slot t, the sixth and seventh cases correspond to that a collision occurs.

D. Computing $(\hat{f}_{t+1,w,g})_{w,g\in\mathbb{N}}$ Using the Update Generation Probability

It remains to obtain $(\hat{f}_{t+1,w,g})_{w,g\in\mathbb{N}}$ at the beginning of slot $t+1$ based on $(\hat{f}_{t^+,w,g})_{w,g\in\mathbb{N}}$ and the update generation probability λ. Initially, for each $n \in \mathcal{N}$, each device knows $h_{n,0} = w_{n,0} = g_{n,0} = 0$, which implies

$$\hat{f}_{0,w,g} = \begin{cases} 1, & \text{if } w = g = 0, \\ 0, & \text{otherwise.} \end{cases} \tag{38}$$

Considering that each device independently generates an update with probability λ at the beginning of each frame m (i.e., $t = mD, m \in \mathbb{Z}^+$) and does not generate updates at other time points, we have

$$\begin{aligned} \hat{f}_{t+1,w',g'} &\triangleq \Pr\big(w_{n,t+1} = w', g_{n,t+1} = g' | \lambda, (\hat{f}_{t^+,w,g})_{w,g\in\mathbb{N}}\big) \\ &= \sum_{w,g\in\mathbb{N}} \hat{f}_{t^+,w,g} \Pr\big(w_{n,t+1} = w', g_{n,t+1} = g' | \lambda, \\ &\qquad w_{n,t^+} = w, g_{n,t^+} = g\big), \end{aligned} \tag{39}$$

for each $t, w', g' \in \mathbb{N}$, where

$$\Pr\big(w_{n,t+1} = w', g_{n,t+1} = g' | \lambda, w_{n,t^+} = w, g_{n,t^+} = g\big) = \begin{cases} \lambda, & \text{if } t = mD-1, m \in \mathbb{Z}^+, w' = 0, g' = w+g, \\ 1-\lambda, & \text{if } t = mD-1, m \in \mathbb{Z}^+, w' = w, g' = g, \\ 1, & \text{if } t \neq mD-1, m \in \mathbb{Z}^+, w' = w, g' = g, \\ 0, & \text{otherwise.} \end{cases} \tag{40}$$

The enhanced T-AGDSA is summarized in Algorithm 1, which, as shown in Fig. 5, can be implemented in a decentralized manner as in [19], [20], since each device only uses its previous action Γ_{t-1}, p_{t-1}, and previous globally available feedback c_{t-1} for determining Γ_t, p_t individually at slot t, without requiring coordination with each other.

E. Impacts of Network Parameters

Obviously, the network parameters have a significant impact on the accuracy of Eq. (33), and thus have a significant impact on the network AAoI improvement through maximizing Eq. (33). A key assumption in deriving Eq. (33) is that the states of all the devices are independent of each other, which would become more reasonable for larger N, smaller λ or larger D. Further, according to Eqs. (39)–(40), as λ is closer to 0 or 1, the estimate of $\hat{f}_{t,w,g}$ would become more accurate due to the reduced uncertainty, thus leading to higher accuracy of Eq. (33). As D increases, there would be more successful transmissions during a frame, and thus more devices would enjoy the zero age gain at more time slots. By this fact and Eqs. (35)–(37), the accuracy of the estimate of age gains increases as D increases, thus increasing the accuracy of Eq. (33). On the other hand, as D increases, each device has a lower frequency of using the packet generation event to reduce its local age to zero, which is also reflected in Eqs. (35)–(37). So, the accuracy of the estimate of local ages would decrease as D increases, especially when λ is large, thus decreasing the accuracy of Eq. (33). Obviously, the accuracy of the independence assumption is more sensitive than that of the

estimate of $\hat{f}_{t,w,g}$ for impacting the accuracy of Eq. (33). So, in general, Eq. (33) has higher accuracy for larger N, smaller λ or larger D, leading to more proper Γ_t, p_t for improving the network AAoI.

Algorithm 1 The proposed enhanced T-AGDSA.

Set $t = 0$.
for each $n \in \mathcal{N}$ **do**
  // Implemented at the beginning of slot t.
  if $t = 0$ **then**
    Device n uses Eq. (38) to obtain $\hat{f}_{0,w,g}$.
  else
    if $t = mD, m \in \mathbb{Z}^+$ **then**
      Device n uses Eq. (39) to obtain $(\hat{f}_{t,w,g})_{w,g\in\mathbb{N}}$.
    else
      Device n obtains $(\hat{f}_{t,w,g})_{w,g\in\mathbb{N}} = (\hat{f}_{(t-1)^+,w,g})_{w,g\in\mathbb{N}}$.
    end if
  end if
  Based on Eq. (34), device n chooses Γ_t and p_t that maximize Eq. (33).
  if $g_{n,t} \geq \Gamma_t$ **then**
    In slot t, device n transmits with probability p_t,
  else
    In slot t, device n keeps silent.
  end if
  // Implemented at the end of slot t.
  Device n obtains the channel status c_t.
  Device n uses Eq. (35) to obtain $(\hat{f}_{t^+,w,g})_{w,g\in\mathbb{N}}$.
end for
$t = t + 1$, return to step 2.

F. Complexity Analysis

The enhanced T-AGDSA has no need for offline computation but has an online computational complexity $\mathcal{O}(\frac{U^2}{D^2}) + \mathcal{O}(N^2)E_{\text{1search}}$ in each slot t because the maximum number of non-zero elements of either of $(\hat{f}_{t,w,g})_{w,g\in\mathbb{N}}$ and $(\hat{f}_{t^+,w,g})_{w,g\in\mathbb{N}}$ is $\frac{U^2}{D^2}$, each of which has at most two nonzero-probability transitions in either of Eqs. (37) and (40). Here E_{1search} denotes the number of the evaluations of Eq. (33) for searching $\hat{\Gamma}_t^o$ and $E_{\text{1search}} \leq \mathcal{O}(\frac{U}{D})$. Since the function $\hat{R}_t(\Gamma_t, \hat{p_t^o})$ is unimodal in our implementation, we can use the bisection search method to obtain $E_{\text{1search}} \leq \mathcal{O}(log_2 \frac{U}{D})$.

One can see Section III-F for comparing both the offline and online complexity of the basic and the enhanced T-AGDSA.

Remark 8: It is difficult to use the current framework to provide analytical tractability of the enhanced-TAGDSA, where the curse of dimensionality of the underlying belief $(\hat{f}_{t,w,g})_{w,g\in\mathbb{N}}$ is one of the major causes. This is a common weakness in adaptive-threshold schemes [19], [20], which thus restricted their computation to beliefs that are actually reached as done in our work. One possible solution is to apply the belief compression and clustering technique in the context of partially observable Markov decision processes [34].

V. Numerical Results

This section consists of three subsections. The first subsection validates the analytical modeling of the proposed basic T-AGDSA and examines its advantage over the following schemes with fixed access parameters.

(i) Optimal slotted ALOHA [22], [23], [25]: under the age gain threshold $\Gamma_t = 1$, each device uses an optimal fixed p_t. Note that [25] only considered $\lambda = 1$ and [22], [23] only considered $D = 1$, so we will obtain the network AAoI for other cases via simulations.

(ii) Threshold-ALOHA for $D = 1$ [11]: each device uses an optimal fixed Γ_t and an optimal fixed p_t when $\lambda = D = 1$, and uses an suboptimal fixed Γ_t and an suboptimal fixed p_t when $\lambda < 1$, $D = 1$.

The second subsection examines the advantage of the proposed enhanced T-AGDSA over the following schemes with adaptive access parameters.

(i) Ideal scheduling [19]: the AP always selects one of the devices with the highest age gains to transmit. It provides a lower bound on the network AAoI.

(ii) Ideal adaptive slotted ALOHA [25]: each device uses $p_t = 1/n_t$ and $\Gamma_t = 1$, where n_t represents the number of active devices in slot t.

(iii) AAT [19] for $D = 1$: see Section I-B for details.

(iv) T-DFSA [20] for $D = 1$: see Section I-B for details.

The third subsection compares the basic T-AGDSA and enhanced T-AGDSA. The scenarios considered in the simulations are in accordance with the descriptions in Section II. We shall vary the network configuration over a wide range to validate our theoretical study. Each simulation result is obtained from 10 independent simulation runs with 10^7 slots in each run.

A. Basic T-AGDSA

Fig. 6 shows the network AAoI of the basic T-AGDSA as a function of the update generation probability λ for different N and D. Note that the threshold-ALOHA [11] is inapplicable when $D > 1$. The curves indicate that our analytical modeling is accurate in all the cases.

1) Impact of the network parameters: We observe that the network AAoI of all the schemes first decreases with λ and then remains almost the same. This is because larger λ is helpful to reduce the AAoI due to the delivery of fresher updates, but this effect would become weaker due to severer contention when λ is larger. We observe that the network AAoI of all the schemes increases with N. This is because the contention among devices is severer with large N. We observe that the network AAoI of optimal slotted ALOHA [25] first keeps almost the same as D increases when D is small and then increases with D when D becomes larger, while the AAoI of basic T-AGDSA always increases with D. This is because introducing the fixed threshold Γ^{sta} prioritizes those devices with large age gains to transmit with less collisions, which mitigates the severe contention caused by small D.

2) Performance comparison: For the case $D = 1$, we observe from Fig. 6(a) that the proposed basic T-AGDSA enjoys up to 47.21% improvement over the optimal slotted

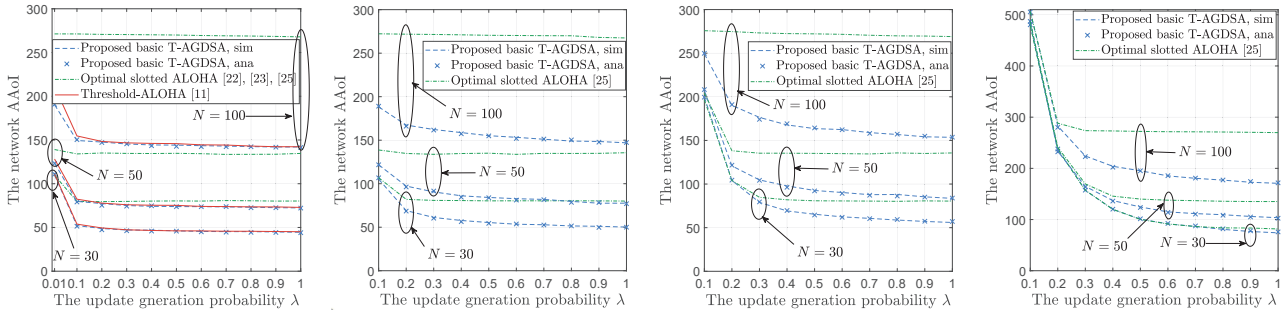

(a) $D = 1$. (b) $D = 10$. (c) $D = 20$. (d) $D = 50$.

Fig. 6. The network AAoI of the proposed basic T-AGDSA versus λ for different N and D.

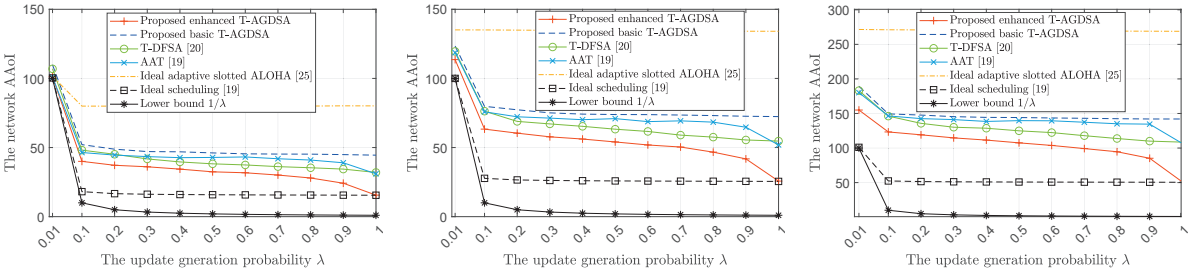

(a) $N = 30$. (b) $N = 50$. (c) $N = 100$.

Fig. 7. The network AAoI of the proposed enhanced T-AGDSA versus λ for different N when $D = 1$.

ALOHA [22], [23], [25], which verifies the benefit of introducing the fixed threshold Γ^{sta}. We also observe the basic T-AGDSA enjoys up to 10.24% improvement over the threshold-ALOHA [11] in large-scale networks with sporadic individual traffic (i.e., when N is large and λ is small), but performs almost the same in other cases. This is because the age gain threshold is more helpful in reducing the AAoI compared with the AoI threshold used in the threshold-ALOHA [11] and this advantage is notable when N is large and λ is small. This advantage is enlarged when λ is small because the threshold-ALOHA [11] used the assumption of $\lambda = 1$ to obtain the transmission policy when $\lambda < 1$.

For the case $D > 1$, we observe from Fig. 6(b)–(d) that, compared with optimal slotted ALOHA [25], the basic T-AGDSA enjoys up to 44.31% improvement when $D = 10$, up to 41.52% improvement when $D = 20$, and up to 35.70% improvement when $D = 50$. These results indicate that introducing Γ^{sta} is effective in improving the AAoI for a wide range of configurations. In conjunction with Fig. 6(a), we further observe that, in general, the advantage of the basic T-AGDSA diminishes when λ decreases, N decreases, or D increases. This is because the effect of introducing Γ^{sta} to mitigate the contention becomes weaker in these cases.

B. Enhanced T-AGDSA

Figs. 7–8 show the network AAoI of the enhanced T-AGDSA as a function of λ for different N and D. Note that AAT [19] and T-DFSA [20] are both inapplicable when $D > 1$.

1) Impact of the network parameters: We observe that the network AAoI of the ideal adaptive slotted ALOHA [25] first decreases with λ and then remains almost the same, while the other schemes always decrease with λ due to the effect of introducing the adaptive age gain threshold. We also observe that the network AAoI of all the schemes increases with N, which indicates again that large N would lead to severer contention. We further observe that the network AAoI of the ideal adaptive slotted ALOHA [25] first keeps almost the same as D increases when D is small and then increases with D when D becomes larger, while the AAoI of the enhanced T-AGDSA and ideal scheduling schemes always increases with D. This verifies the benefit of introducing the adaptive threshold to prioritize the devices with large gains.

2) Performance comparison: For the case $D = 1$, we observe from Fig. 7 that the enhanced T-AGDSA enjoys up to 81.06% improvement over the ideal adaptive slotted ALOHA [25]. This verifies the benefit of introducing the adaptive threshold Γ_t, even if the latter utilizes the ideal knowledge of n_t. We also observe from Fig. 7 that the enhanced T-AGDSA enjoys up to 52.21% improvement over the AAT [19], and enjoys up to 53.07% improvement over the T-DFSA [20]. This is owing to our more reasonable Γ_t, which is computed by not only a more accurate estimation of the age gains (see Remark 6) but also a more reasonable optimization goal (see Remarks 4 and 5). We further observe that all the schemes in Fig. 7 enjoy almost the same AAoI (close to $1/\lambda$) when $N\lambda$ is small, which confirms the lower bound $1/\lambda$ proposed in [19]. This is because the inter-arrival time becomes a dominant factor in determining the AAoI when the network traffic is quite low. On the other hand, when $N\lambda$ is not small, we note that the enhanced T-AGDSA performs closer to the ideal scheduling [19] as λ increases, which implies that

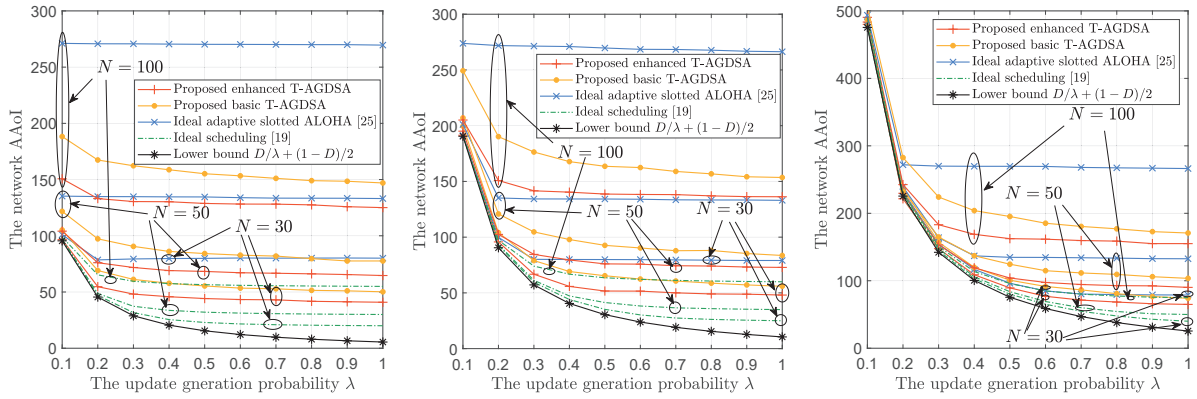

(a) $D = 10$. (b) $D = 20$. (c) $D = 50$.

Fig. 8. The network AAoI of the proposed enhanced T-AGDSA versus λ for different N when $D > 1$.

our adaptive threshold can be chosen to limit the contention to fewer devices with higher age gains due to a more accurate estimation of age gains.

For the case $D > 1$, we observe from Fig. 8 that, compared with the ideal adaptive slotted ALOHA [25], the enhanced T-AGDSA enjoys up to 53.61% improvement when $D = 10$, up to 48.85% improvement when $D = 20$, and up to 41.79% improvement when $D = 50$. These results indicate that introducing the adaptive Γ_t is effective in improving the AAoI for a wide range of configurations. In conjunction with Fig. 7, we also observe that, in general, such improvement diminishes when λ decreases, N decreases, or D increases. This is because the effect of introducing the adaptive Γ_t to mitigate the contention becomes weaker in these cases. We further observe that all the schemes enjoy almost the same AAoI (close to D/λ) when $N\lambda/D$ is small, which confirms our proposed lower bound $D/\lambda + (1 - D)/2$. We also note that the AAoI of the enhanced T-AGDSA always decreases with λ when $D = 1$, but first decreases with λ and then keeps almost the same when $D > 1$. This is because there would be more devices with large age gains as D increases, which leads to severer contentions that weaken the advantage of more accurate estimation of age gains under larger λ.

C. Basic T-AGDSA V.S. Enhanced T-AGDSA

We observe from Figs. 7–8 that, compared with the proposed basic T-AGDSA, the proposed enhanced T-AGDSA enjoys $7.81\% - 64.98\%$ improvement when $D = 1$, $8.19\% - 21.36\%$ improvement when $D = 10$, $3.08\% - 20.17\%$ improvement when $D = 20$, and $0.04\% - 18.32\%$ improvement when $D = 50$. As expected, we note that such improvement is close to zero when $N\lambda/D$ is quite low. We also observe that such improvement always increases with λ when $D = 1$, but first increases with λ and then decreases with λ when $D > 1$. This indicates again that increased D diminishes the advantage of the enhanced T-AGDSA. Such improvement comes from more reasonable setting of the age gain threshold, but at a cost of higher online computation burden on each device.

VI. Conclusion

In this paper, we have investigated how to design decentralized schemes for reducing the network AAoI in an uplink IoT system with event-driven periodic updating, so that the unavoided contention can be limited to devices with age gains as high as possible. We proposed a basic T-AGDSA scheme, where the access parameters are fixed and can be obtained offline using the proposed multi-layer Markov modeling approach. We then proposed an enhanced T-AGDSA scheme, where each device adjusts the access parameters to maximize the estimated network EAR per slot, built on an estimation of the joint probability distribution of local age and age gain of an arbitrary device. Numerical results validated our theoretical study and confirmed the advantage of our proposed schemes over the existing schemes. Compared with [10]–[25], our work provides handy tools to design AGDRA schemes of practical communication systems in more general scenarios. Our work indicates that how to obtain and how to utilize the knowledge of age gains properly are both essential, and the performance-complexity tradeoff needs to be considered in practice.

Synchronous traffic and instantaneous error-free ACKs are two key assumptions in our work. To extend the applicability, our future work will relax the former to investigate how to model heterogeneous behaviors to derive Eq. (18) for designing basic T-AGDSA and how to apply multi-agent deep reinforcement learning (MARL) algorithms to cope with asymmetric age gain beliefs for designing enhanced T-AGDSA. We will also relax the latter to investigate how to incorporate additional states to capture the estimated age gain for designing basic T-AGDSA and how to modify the MARL algorithm with feedback recovery [35] for designing enhanced T-AGDSA. Another future direction is to examine the performance of the proposed schemes in practical systems.

Appendix
Proof of Proposition 1

Suppose that each update can be instantaneously delivered without experiencing collisions. Let $I_{n,i}$ denote the inter-arrival time between the $(i-1)$-th and i-th updates of the tagged device n, which is obviously equal to the inter-delivery

time. Considering that each device independently generates an update with probability λ at the beginning of each frame and does not generate updates at other time points, we have

$$\Pr\big(I_{n,i} = jD\big) = (1-\lambda)^{j-1}\lambda, \tag{41}$$

for $i = 1, 2, \ldots$, and $j = 1, 2, \ldots$.

Since $I_{n,i}/D$ in Eq. (41) has a geometric distribution with parameter λ, we have

$$\mathbb{E}(I_{n,i}) = D\mathbb{E}(I_{n,i}/D) = D/\lambda, \tag{42}$$

$$\mathbb{E}(I_{n,i}^2) = D^2\mathbb{E}\big((I_{n,i}/D)^2\big) = D^2(2-\lambda)/\lambda^2. \tag{43}$$

Let $\zeta_{n,T}$ be the number of successfully transmitted updates of device n until the T-th slot. The AAoI of device n defined in Eq. (3) can be rewritten as

$$\begin{aligned}\Delta_n &= \lim_{T\to\infty} \frac{\zeta_{n,T}}{T}\frac{1}{\zeta_{n,T}}\sum_{i=1}^{\zeta_{n,T}}\sum_{h=1}^{I_{n,i}} h \\ &= \lim_{T\to\infty} \frac{\zeta_{n,T}}{T}\frac{1}{\zeta_{n,T}}\sum_{i=1}^{\zeta_{n,T}}\big(I_{n,i}(I_{n,i}+1)/2\big) \\ &= \frac{\mathbb{E}\big(I_{n,i}(I_{n,i}+1)/2\big)}{\mathbb{E}(I_{n,i})} = \frac{\mathbb{E}(I_{n,i}^2)}{2\mathbb{E}(I_{n,i})} + 1/2. \end{aligned} \tag{44}$$

By substituting Eqs. (42) and (43) into Eq. (44), we can obtain

$$\Delta_n = \frac{D^2(2-\lambda)/\lambda^2}{2D/\lambda} + \frac{1}{2} = D/\lambda + (1-D)/2, \tag{45}$$

which can be served as a lower bound.

REFERENCES

[1] M. Bennis, M. Debbah, and H. V. Poor, "Ultrareliable and low-latency wireless communication: Tail, risk, and scale," *Proc. IEEE*, vol. 106, no. 10, pp. 1834–1853, Sep. 2018.

[2] Z. Ma, M. Xiao, Y. Xiao, Z. Pang, H. V. Poor, and B. Vucetic, "High-reliability and low-latency wireless communication for Internet of Things: Challenges, fundamentals, and enabling technologies," *IEEE Internet Things J.*, vol. 6, no. 5, pp. 7946–7970, Mar. 2019.

[3] M. Luvisotto, Z. Pang, and D. Dzung, "High-performance wireless networks for industrial control applications: New targets and feasibility," *Proc. IEEE*, vol. 107, no. 6, pp. 1074–1093, Mar. 2019.

[4] S. Kaul, M. Gruteser, V. Rai, and J. Kenney, "Minimizing age of information in vehicular networks," in *Proc. IEEE SECON*, Salt Lake City, Jun. 2011, pp. 350–358.

[5] A. Gong, T. Zhang, H. Chen, and Y. Zhang, "Age-of-information-based scheduling in multiuser uplinks with stochastic arrivals: A POMDP approach," in *Proc. IEEE GLOBECOM*, Taipei, Dec. 2020, pp. 1–6.

[6] R. Talak, S. Karaman, and E. Modiano, "Optimizing information freshness in wireless networks under general interference constraints," *IEEE/ACM Trans. Netw.*, vol. 28, no. 1, pp. 15–28, Dec. 2020.

[7] A. Maatouk, S. Kriouile, M. Assad, and A. Ephremides, "On the optimality of the Whittle's index policy for minimizing the age of information," *IEEE Trans. Wirel. Commun.*, vol. 20, no. 2, pp. 1263–1277, Oct. 2021.

[8] I. Kadota and E. Modiano, "Minimizing the age of information in wireless networks with stochastic arrivals," *IEEE Trans. Mob. Comput.*, vol. 20, no. 3, pp. 1173–1185, Dec. 2021.

[9] M. J. Kochenderfer, *Decision making under uncertainty: Theory and application*. MIT Press, Jan. 2015.

[10] D. C. Atabay, E. Uysal, and O. Kaya, "Improving age of information in random access channels," in *Proc. IEEE INFOCOM Workshops*, Toronto, Jul. 2020, pp. 912–917.

[11] O. T. Yavascan and E. Uysal, "Analysis of slotted ALOHA with an age threshold," *IEEE J. Sel. Areas Commun.*, vol. 39, no. 5, pp. 1456–1470, Mar. 2021.

[12] H. Chen, Y. Gu, and S.-C. Liew, "Age-of-information dependent random access for massive IoT networks," in *Proc. IEEE INFOCOM Workshops*, Toronto, Jul. 2020, pp. 930–935.

[13] M. Ahmetoglu, O. T. Yavascan, and E. Uysal, "Mista: An age-optimized slotted ALOHA protocol," *IEEE Internet Things J.*, vol. 9, no. 17, pp. 15484–15496, May 2022.

[14] O. T. Yavascan, M. Ahmetoglu, and E. Uysal, "Mumista: An age-aware reservation-based random access policy," in *Proc. IEEE WiOpt*, Singapore, Aug. 2023, pp. 597–602.

[15] Y. Zhu, W. Zhang, Y. Lin, Y.-H. Lo, and Y. Zhang, "Improving age of information in large-scale energy harvesting networks," in *Proc. IEEE ICC Workshops*, Rome, May 2023, pp. 1173–1178.

[16] H. H. Yang, N. Pappas, T. Q. S. Quek, and M. Haenggi, "Analysis of the age of information in age-threshold slotted ALOHA," in *Proc. IEEE WiOpt*, Singapore, Mar. 2023, pp. 366–373.

[17] H. Xie, Y. Hu, S.-W. Jeon, and H. Jin, "Random activation control for priority AoI," in *Proc. IEEE CCNC*, Las Vegas, Jan. 2023, pp. 443–448.

[18] J. Sun, Z. Jiang, B. Krishnamachari, S. Zhou, and Z. Niu, "Closed-form Whittle's index-enabled random access for timely status update," *IEEE Trans. Commun.*, vol. 68, no. 3, pp. 1538–1551, Dec. 2020.

[19] X. Chen, K. Gatsis, H. Hassani, and S. S. Bidokhti, "Age of information in random access channels," *IEEE Trans. Inf. Theory*, vol. 68, no. 10, pp. 6548–6568, Jun. 2022.

[20] M. Moradian, A. Dadlani, A. Khonsari, and H. Tabassum, "Age-aware dynamic frame slotted ALOHA for machine-type communications," *IEEE Trans. Commun.*, vol. 72, no. 5, pp. 2639–2654, Jan. 2024.

[21] P. Mollahosseini, S. Asvadi, and F. Ashtiani, "Effect of variable backoff algorithms on age of information in slotted ALOHA networks," *IEEE Trans. Mob. Comput.*, pp. 1–14, Jan. 2024.

[22] R. D. Yates and S. K. Kaul, "Status updates over unreliable multiaccess channels," in *Proc. IEEE ISIT*, Aachen, Jun. 2017, pp. 331–335.

[23] I. Kadota and E. Modiano, "Age of information in random access networks with stochastic arrivals," in *Proc. IEEE INFOCOM*, Vancouver, May 2021, pp. 1–10.

[24] J. Wang, J. Yu, X. Chen, L. Chen, C. Qiu, and J. An, "Age of information for frame slotted ALOHA," *IEEE Trans. Commun.*, vol. 71, no. 4, pp. 2121–2135, Jan. 2023.

[25] Y. H. Bae and J. W. Baek, "Age of information and throughput in random access-based IoT systems with periodic updating," *IEEE Wirel. Commun. Lett.*, vol. 11, no. 4, pp. 821–825, Jan. 2022.

[26] A. Fu and M. Mazo, "Traffic models of periodic event-triggered control systems," *IEEE Trans. Autom. Control*, vol. 64, no. 8, pp. 3453–3460, Nov. 2019.

[27] L. Deng, F. Liu, Y. Zhang, and W. S. Wong, "Delay-constrained topology-transparent distributed scheduling for MANETs," *IEEE Trans. Veh. Technol.*, vol. 70, no. 1, pp. 1083–1088, Dec. 2021.

[28] D. Feng, C. She, K. Ying, L. Lai, Z. Hou, T. Q. S. Quek, Y. Li, and B. Vucetic, "Toward ultrareliable low-latency communications: Typical scenarios, possible solutions, and open issues," *IEEE Veh. Technol. Mag.*, vol. 14, no. 2, pp. 94–102, Apr. 2019.

[29] Z. Jiang, B. Krishnamachari, S. Zhou, and Z. Niu, "Can decentralized status update achieve universally near-optimal age-of-information in wireless multiaccess channels?" in *Proc. ITC 30*, vol. 01, Austria, Sep. 2018, pp. 144–152.

[30] G. N. Grapiglia and F. Chorobura, "Worst-case evaluation complexity of derivative-free nonmonotone line search methods for solving nonlinear systems of equations," *Comput. Appl. Math.*, vol. 40, Dec. 2021.

[31] J. Larson, M. Menickelly, and S. Wild, "Derivative-free optimization methods," *Acta Numerica*, vol. 28, pp. 287–404, May 2019.

[32] R. Rivest, "Network control by Bayesian broadcast," *IEEE Trans. Inf. Theory*, vol. 33, no. 3, pp. 323–328, Jan. 1987.

[33] T. N. Weerasinghe, V. Casares-Giner, I. A. M. Balapuwaduge, F. Y. Li, and M.-C. Vochin, "A pseudo-Bayesian subframe based framework for grant-free massive random access in 5G NR networks," in *Proc. IEEE ICCCN*, Honolulu, Jul. 2022, pp. 1–7.

[34] X. Li, W. K. Cheung, and J. Liu, "Improving POMDP tractability via belief compression and clustering," *IEEE Trans. Syst., Man, Cybern. B*, vol. 40, no. 1, pp. 125–136, Jul. 2010.

[35] Y. Yu, S. C. Liew, and T. Wang, "Multi-agent deep reinforcement learning multiple access for heterogeneous wireless networks with imperfect channels," *IEEE Trans. Mob. Comput.*, vol. 21, no. 10, pp. 3718–3730, Feb. 2022.

Yuqing Zhu received the B.S. degree in communication engineering from the Nanjing University of Science and Technology, Nanjing, China, in 2023, where she is currently pursuing the Ph.D. degree with the School of Electronic and Optical Engineering. Her research focuses on multiple access for communication systems.

Yiwen Zhu received the B.S. degree in communication engineering from the Nanjing University of Science and Technology, Nanjing, China, in 2022, where she is currently pursuing the M.S. degree with the School of Electronic and Optical Engineering. Her research focuses on multiple access for communication systems.

Aoyu Gong received the B.E. degree in communication engineering from Nanjing University of Science and Technology, Nanjing, China, in 2019, and the M.S. degree in communication systems from École Polytechnique Fédérale de Lausanne, Lausanne, Switzerland, in 2024, where he is currently pursuing the Ph.D. degree with the School of Computer and Communication Sciences. His research focuses on low-latency solutions for next-generation wireless networks.

Yan Lin (Member, IEEE) received the M.S. and Ph.D. degrees from Southeast University, China, in 2013 and 2018, respectively. She visited the Southampton Wireless Group, Southampton University, U.K., from October 2016 to October 2017. She joined the Nanjing University of Science and Technology, China, in 2018, where she is currently an Associate Professor with the School of Electronic and Optical Engineering. Her current research interests include vehicular networks, UAV networks, mobile edge computing, and reinforcement learning for resource allocation in wireless communication.

Yuan-Hsun Lo (Member, lEEE) received the B.S., M.S., and Ph.D. degrees in applied mathematics from National Chiao Tung University, Hsinchu. Taiwan, in 2004, 2006, and 2010, respectively. He has been with Xiamen University since 2015. Then, he joined National Pingtung University, Taiwan, in 2019, where he is currently a Professor with the Department of Applied Mathematics. His research interests include combinatorics, graph theory, and combinatorial designs and their applications.

Yijin Zhang (Senior Member, IEEE) received the B.S. degree in information engineering from the Nanjing University of Posts and Telecommunications, China, in 2004, the M.S. degree in information engineering from Southeast University, China, in 2007, and the Ph.D. degree in information engineering from The Chinese University of Hong Kong in 2010. He joined the Nanjing University of Science and Technology, China, in 2011, where he is currently a Professor with the School of Electronic and Optical Engineering. His current research interests include sequence design and resource allocation for communication networks.